Published in final edited form as:
IEEE J Sel Top Quantum Electron. 2012 ; 18(3): . doi:10.1109/JSTQE.2011.2168559.

Multimodal Nonlinear Microscopy by Shaping a Fiber Supercontinuum From 900 to 1160 nm

Yuan Liu
Department of Bioengineering, Biophotonics Imaging Laboratory, Beckman Institute for Advanced Science and Technology, University of Illinois at Urbana-Champaign, Urbana, IL 61801 USA (yuanliu3@illinois.edu)

Haohua Tu
Biophotonics Imaging Laboratory, Beckman Institute for Advanced Science and Technology, University of Illinois at Urbana-Champaign, Urbana, IL 61801 USA (htu@illinois.edu)

Wladimir A. Benalcazar
Department of Physics, Biophotonics Imaging Laboratory, Beckman Institute for Advanced Science and Technology, University of Illinois at Urbana-Champaign, Urbana, IL 61801 USA (wbenalc2@illinois.edu)

Eric J. Chaney
Biophotonics Imaging Laboratory, Beckman Institute for Advanced Science and Technology, University of Illinois at Urbana-Champaign, Urbana, IL 61801 USA (echaney@illinois.edu)

Stephen A. Boppart [Fellow, IEEE]
Departments of Electrical and Computer Engineering, Bioengineering, and Medicine, Biophotonics Imaging Laboratory, Beckman Institute for Advanced Science and Technology, University of Illinois at Urbana-Champaign, Urbana, IL 61801 USA (boppart@illinois.edu)

Abstract

Nonlinear microscopy has become widely used in biophotonic imaging. Pulse shaping provides control over nonlinear optical processes of ultrafast pulses for selective imaging and contrast enhancement. In this study, nonlinear microscopy, including two-photon fluorescence, second harmonic generation, and third harmonic generation, was performed using pulses shaped from a fiber supercontinuum (SC) spanning from 900 to 1160 nm. The SC generated by coupling pulses from a Yb:KYW pulsed laser into a photonic crystal fiber was spectrally filtered and compressed using a spatial light modulator. The shaped pulses were used for nonlinear optical imaging of cellular and tissue samples. Amplitude and phase shaping the fiber SC offers selective and efficient nonlinear optical imaging over a broad bandwidth with a single-beam and an easily tunable setup.

Keywords

Biomedical imaging; biophotonics; nonlinear optics; optical microscopy; supercontinuum (SC) generation

I. Introduction

NONLINEAR microscopy has emerged as a powerful technique in biophotonic imaging. Several modalities, such as two-photon fluorescence (TPF) [1], second harmonic generation (SHG) [2], and third harmonic generation (THG) [3] microscopy, have been investigated and applied in biomedical research. Because of the nonlinear processes and longer laser

wavelength, these modalities generally provide the advantages of 3-D localized excitation and separate excitation and emission spectra, reduced photodamage, and deeper penetration [4]–[6].

Coherent control enables engineering of light–matter interactions to extract more information in nonlinear optical microscopy and spectroscopy [7]–[9]. Control of two-photon excitation by shaping femtosecond laser pulses has been demonstrated [10], [11]. Sinusoidal phase shaping [12], binary phase shaping [13], antisymmetric phase shaping [14], and adaptive phase shaping [15] of ultrafast pulses have been demonstrated to selectively image fluorophores in biological samples. While phase-only shaping techniques have been studied extensively in TPF imaging, the potential of amplitude shaping has not been fully utilized. Amplitude shaping to select the fundamental excitation spectra is practically robust and simple, and phase shaping in addition can compensate the dispersion to higher order to enhance the excitation efficiency [16], [17]. To date, pulse shaping techniques have not found wide applications in SHG and THG imaging [18], [19]. This method can also be applied for SHG and THG imaging with arbitrary spectral range within the fundamental spectrum to improve efficiency.

Supercontinuum (SC) generation by pumping a photonic crystal fiber (PCF) with laser pulses offers an alternative broadband light source to mode-locked solid-state lasers [20]. The ultrabroad bandwidth and versatility of a PCF as an add-on to a solid-state laser makes it appealing for biophotonic imaging. Fiber SC has been utilized in TPF microscopy. Improved TPF efficiency using a compressed SC [21], short-wavelength TPF imaging [22], simultaneous excitation of multiple fluorophores [23], and selective excitation by spectrally filtering an SC [24] have been reported. The combination of an SC source and pulse shaping can offer control of two-photon excitation over an ultrabroad spectral range. Adaptive pulse shaping of the excitation source to achieve selective flurophore excitation has been demonstrated [25]. However, pulse shaping of SC for TPF, SHG, and THG imaging of biological samples has not been shown.

In this study, nonlinear optical imaging by amplitude and phase shaping a fiber SC from 900 to 1160 nm is demonstrated. The SC generated by pumping a PCF was spectrally filtered and compressed by a pulse shaper to perform TPF, SHG, and THG imaging of biological samples. Selective and efficient TPF imaging of fluorophores was achieved, as shown by comparing images with different excitation control. Improved efficiency of SHG and THG imaging was also demonstrated by pulse compression.

II. Experiments

The experimental setup is shown in Fig. 1. Pulses from a Yb:KYW laser (femtoTRAIN IC-1040-3000, High Q Laser, Austria) of 1040 nm, 76 MHz were coupled into a highly nonlinear PCF (NL-1050-NEG-1, NKT Photonics, Denmark) for SC generation. Details about the fiber SC can be found in our other studies [26]–[28]. The SC was collimated by a parabolic mirror and modulated by a multiphoton intrapulse interference phase scan (MIIPS)-assisted 4-f pulse shaper, which allows amplitude and phase shaping from 700 to 1350 nm over a 640-pixel liquid crystal (MIIPS Box 640, Biophotonics Solutions). The SC was guided into an upright microscope (BX61WI, Olympus) modified for nonlinear optical imaging. A dichroic mirror (T700spxc-1500, Chroma Technology, VT) reflected the SC into an objective (LUMPLFL60XW/IR2, NA = 0.9, Olympus) and transmitted the backward nonlinear optical signal from the samples. Imaging was performed by scanning a motorized stage (Bioprecision, Ludl Electronic Products). The nonlinear optical signal was detected by a photomultiplier tube (H7421-40, Hamamatsu, Japan) after passing a bandpass filter wheel. The SHG signal generated from a 10-μm-think beta barium borate (BBO) crystal was

acquired in the forward direction by a spectrometer (USB4000, Ocean Optics) to perform MIIPS scans, for *in situ* pulse measurement and dispersion compensation [29].

Our pulse shaping strategy was to obtain transform-limited (TL) pulses of different spectral ranges for selective and efficient nonlinear optical imaging. First, amplitude shaping was used to select the fundamental spectra by blocking undesired wavelengths, as illustrated by the shaded areas in Fig. 2. The selected bands of 930–990 nm and 1100–1160 nm were designated as green uncompressed and red uncompressed pulses, respectively. Second, phase shaping was used to compress the pulses by compensating the dispersion measured at the focus of the objective, as illustrated by the color dashed lines in Fig. 2. The SC spectral phase measurement and pulse compression to the TL were discussed in [27] and [28]. The compressed pulses spanning the spectral ranges of 930–990 nm and 1100–1160 nm were designated as green compressed and red compressed pulses, respectively.

The mitochondria of mouse green fluorescent protein (GFP)-transfected 3T3 fibroblasts were labeled with Mitotracker Red CMXRos (M7512, Invitrogen) at a concentration of 100 nM for 15 min. Excess dye was then washed off and replaced by culture medium before TPF imaging. The two-photon excitation spectra of fluorophores were used to determine the pulses used for selective excitation. GFP can be excited by green pulses from 930 to 990 nm [30]; and Mitotracker Red CMXRos can be excited by red pulses from 1100 to 1160 nm [31].

The SC power was controlled by a neutral density filter before entering the microscope and prior to amplitude shaping. The imaging power under the objective in the GFP channel (520 ± 17 nm) was 3.1 mW for green pulses and 7.5 mW for red pulses. The power in the red channel (620 ± 26 nm) was 0.6 mW for green pulses and 1.4 mW for red pulses. Because only phase shaping was performed to compress the spectrally filtered pulses, the average power was the same when imaging with compressed and uncompressed pulses. Different power levels were employed in the two channels due to the different sensitivity of targeted fluorophores and detection bandwidths.

Frozen porcine skin was cut to 100-μm-thick cross sections and thawed before label-free multimodal nonlinear optical imaging. Green pulses, the short-wavelength end of the SC, were used in TPF imaging in order to excite endogenous fluorescent biomolecules. Red pulses, the long-wavelength end of the SC, were used to avoid excitation crosstalk of TPF in SHG imaging and to have better detection quantum efficiency in THG imaging. Different bandpass filters were employed in front of the photomultiplier tube for acquiring different signals (TPF: 542 ± 25 nm, SHG: 562 ± 40 nm, THG: 376 ± 20 nm). The imaging under the objective for TPF, SHG, and THG were 3.3, 1.7, and 9 mW, respectively. These power levels provided sufficient signal without saturating the photomultiplier tube for each modality.

III. Results

The SHG spectra of green/red and compressed/uncompressed pulses are shown in Fig. 3 for evaluating their two-photon excitation spectra. The SHG spectral ranges were limited by their fundamental spectra as controlled by amplitude shaping. The spectra are normalized to the maximal SHG intensity of compressed pulses in each color. By pulse compression, the SHG intensity within the desired spectral ranges was improved by 4.4- and 2.8-fold for green and red pulses, respectively.

TPF images of the cell samples from different detection channels (row) illuminated with different colors of compressed pulses (columns) are shown in Fig. 4. In the GFP channel, the fluorescence signal from green compressed pulses is clearly seen while that from red

compressed pulses is not observable. In the red channel, the fluorescence signal from red compressed pulses is clearly seen while that from green compressed pulses is relatively weak. This weak signal has similar spatial distribution as that in the GFP channel and can be identified as emission crosstalk from the GFP fluorescence. The images in the same channels are represented with the same normalized contrast. These results demonstrate selective two-photon excitation of GFP and Mitotracker Red CMXRos by green and red compressed pulses, respectively.

TPF images of the cell samples illuminated by compressed and uncompressed pulses are compared in Fig. 5. Images in which fluorophores were selectively excited are combined for illustration. Fig. 5(a) is merged from the image of green compressed pulses in the GFP channel and from red compressed pulses in the red channel. Fig. 5(b) shows the uncompressed control. The fluorescence signal from compressed pulses is significantly improved compared to that from uncompressed pulses. The improvement of fluorescence intensity within the entire cellular area is calculated to be 3.6- and 3.2-fold for green and red signals, respectively.

Label-free multimodal nonlinear optical images of porcine skin cross sections illuminated by compressed and uncompressed pulses are compared in Fig. 6(a) and (b). TPF, SHG, and THG signals are represented in red, green, and blue pseudocolors. All of the nonlinear optical signals from compressed pulses were greatly improved compared to those from uncompressed pulses. The improvement of TPF, SHG, and THG signals was calculated to be 1.9-, 2.4-, and 8.5-fold, respectively. TPF emission was strongest from the stratum corneum (left) and from collagen in the papillary dermis and reticular dermis (right) [32]. SHG also showed the collagen structure, as expected, in the papillary dermis and reticular dermis. THG revealed optical inhomogeneities, mainly coming from the stratum granulosum cells in the epidermis, and the stratum spinosum and stratum basale cells in epidermis–dermis junction [33].

IV. Discussion

While phase shaping alone can tailor two-photon excitation, SHG, and THG spectra from ultrafast laser pulses, amplitude shaping to first spectrally filter desired wavelengths is practically robust and easy to implement as long as the laser power is sufficient. Phase shaping techniques can be sensitive to spectral phase acquired in biological samples, thus deteriorating the excitation selectivity [34]. Amplitude shaping does not need a complex spectral phase, which requires expertise in coherent control theory [35] and frequently employs an adaptive algorithm that can be time-consuming when adapting to different biological systems [15]. The total power of our SC before entering the microscope was 100 mW, which is more than sufficient for nonlinear optical imaging of biological samples. Fortuitously, amplitude shaping reduces the number of photons sent into the samples, potentially lowering photodamage due to linear absorption.

In addition to amplitude-based spectral filtering, phase shaping to compress pulses to the TL can effectively improve the efficiency of nonlinear optical processes. The enhancement of the TPF signal was more than threefold in the cell imaging experiment. This approach provides higher order dispersion compensation besides group delay dispersion and rapid switching between different excitation without modifying any optical setup, as compared to using bandpass filters [24] or to changing the wavelength of a narrow-band pulsed laser source [36], [37]. Higher order dispersion compensation can significantly improve TPF efficiency for broadband pulses (>30 nm), reduce necessary imaging power, and thus further lower photodamage to biological samples [17], [19]. Fast switching with a programmable shaper can ease alignment tasks and assist image coregistration of fluorophores. The

switching speed is of tens of milliseconds and is limited by the liquid crystal spatial light modulator used in this study (SLM-640-D-NM, CRi). This method can easily be applied to SHG and THG imaging as demonstrated in the tissue imaging experiment (see Fig. 6). The TPF and SHG signal improvement in the skin tissue experiment is lower than that in the cell experiment. This might be due to loss of scattered photons in biological tissue. The THG signal had a greater improvement as compared to the SHG signal. This is likely because THG is a third-order process while SHG is a second-order process. Therefore, pulses with group delay dispersion experienced more attenuation in THG than SHG, as compared to TL pulses.

By spectral filtering and subsequent compression, the maximum group delay needed to compress the selected bandwidth is reduced, compared to that of compression and subsequent spectral filtering. As a result, smoother spectral phase is introduced, providing higher accuracy in phase shaping. This is because a pixilated shaper can only introduce discretized phase, and smaller phase differences between two adjacent pixels can ensure the fidelity of pulse shaping [38].

The Yb:KYW laser-based SC wavelengths span from 900 to 1160 nm, which are centered in the optical window of biological tissue and, thus, suffer little scattering and absorption in tissue imaging. The spectral range provides a longer wavelength two-photon excitation from 450 to 580 nm, filling the gap between Ti:Sa and Cr:forsterite broadband lasers [39]. This spectral range can also be used for SHG and THG imaging with sufficient quantum efficiency for most silicon-based photodetectors. Our ongoing work is to extend the SC bandwidth by increasing the PCF length and/or pumping power and develop it as a useful light source for biophotonic imaging. Several SC sources of similar spectral ranges have been demonstrated in microscopy and spectroscopy applications. The Ti:Sa laser-based SCs have spectra within 600–1000 nm [40]–[42], and the Er:fiber SC has a spectrum from 900 to 1500 nm [43].

V. Conclusion

Multimodal nonlinear optical microscopy in biological samples was performed by amplitude and phase shaping a fiber SC from 900 to 1160 nm. The SC generated by pumping a PCF with pulses from a Yb:KYW laser was spectrally filtered and compressed under a microscope objective by an MIIPS-assisted pulse shaper. By pulse compression, the SHG signal of green (930–990 nm) and red (1100–1160 nm) pulses was enhanced by 4.4- and 2.8-fold, respectively. In a cell imaging experiment, selective TPF imaging of fluorophores and improved fluorescence signals by factors over 3 were demonstrated. In a porcine skin imaging experiment, label-free multimodal nonlinear optical imaging, including TPF, SHG and THG, and improved signal level were shown. Shaping the SC provides selective and efficient TPF imaging over a long-wavelength broadband (450–580 nm) with a single beam and an easily tunable setup. This approach can also be applied for efficient SHG and THG imaging.

Acknowledgments

The authors appreciate the collaborative efforts from High-Q Laser GmbH, Austria, Biophotonic Solutions, Inc., MI, and NKT Photonics, Denmark. We also thank Darold Spillman for his technical and operations support.

This work was supported in part by the National Institutes of Health under Grant NCI R21/R33 CA115536 and Grant RC1 CA147096 ARRA and in part by the National Science Foundation under Grant CBET 08-52658 ARRA and Grant CBET 10-33906. The work of Y. Liu was supported by the Beckman Institute Seed Grant. The work of W. A. Benalcazar was supported by a Beckman Institute Graduate Fellowship.

Biographies

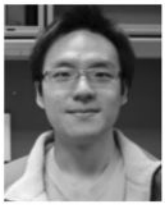

Yuan Liu was born in Taipei, Taiwan, in 1982. He received the B.S. and M.S. degrees in physics from National Taiwan University, Taipei. He is currently working toward the Ph.D. degree in the Department of Bioengineering, Beckman Institute for Advanced Science and Technology, University of Illinois at Urbana-Champaign, Urbana.

His current research interest includes research in the development of nonlinear optical imaging using pulse shaping techniques and coherent control of biological systems.

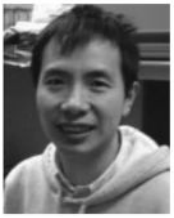

Haohua Tu was born in Wuhan, China, in 1969. He received the B.S. degree in chemical engineering from TsingHua University, Beijing, China, and the Ph.D. degree in chemical engineering and material science from the University of Kentucky, Lexington.

From 2001 to 2005, he was a Postdoctoral Scientist at University of North Carolina, and at University of California-Merced. Since 2005, he has been a Research Scientist at the Biophotonics Imaging Laboratory, Beckman Institute for Advanced Science and Technology, University of Illinois at Urbana-Champaign, Urbana.

Wladimir A. Benalcazar was born in Quito, Ecuador, in 1983. He received the B.S. degree in physics and electrical engineering from Universidad San Francisco de Quito, Quito. He is currently working toward the Ph.D. degree in the Department of Physics, Beckman Institute for Advanced Science and Technology, University of Illinois at Urbana-Champaign, Urbana.

His current research interest includes research in the development of novel optical techniques for assessing molecular and structural information from cells and tissues.

Eric J. Chaney was born in Mount Vernon, IL, in 1970. He received the B.S. degree in biology from the University of Evansville, Evansville, IN, in 1992.

From 1993 to 1997, he was as a Research Assistant at the Indiana University School of Medicine, Indiana State University, Terre Haute. From 1997 to 2000, he was a Transmission Electron Microscope Technician at the University of Illinois at Urbana-Champaign, Urbana. Since 2000, he has been a Research Specialist in molecular biology at the Biophotonics Imaging Laboratory, Beckman Institute for Advanced Science and Technology, University of Illinois at Urbana-Champaign, Urbana.

Stephen A. Boppart (S'90–M'90–SM'06–F'11) was born in Harvard, IL, in 1968. He received the B.S. and M.S. degrees both in electrical engineering from the University of Illinois at Urbana-Champaign, Urbana, in 1990 and 1991, respectively, the Ph.D. degree in electrical and medical engineering from the Massachusetts Institute of Technology, Cambridge, in 1998, and the M.D. degree from Harvard Medical School, Boston, MA, in 2000.

He was a Research Scientist with the Air Force Laser Laboratory, Brooks Air Force Base, San Antonio, TX, where he was involved in research on developing national (ANSI) and Air Force laser safety standards. Since 2000, he has been with the University of Illinois at Urbana-Champaign, from where he completed residency training in internal medicine in 2005. He is currently a Bliss Professor of Engineering in the Departments of Electrical and Computer Engineering, Bioengineering, and Medicine, and the Head of the Biophotonics Imaging Laboratory, Beckman Institute for Advanced Science and Technology, University of Illinois at Urbana-Champaign, and also a Leader of a campus-wide Imaging Initiative. He has authored or coauthored more than 205 invited and contributed publications, and more than 470 invited and contributed presentations. He holds more than 30 patents, filed or pending. His research interests include the development of novel optical imaging technologies for biological and medical applications, with particular emphasis on translating these to clinical applications in cancer detection and diagnosis.

Dr. Boppart is a Fellow of the Optical Society of America and the International Society for Optical Engineering (SPIE). He is a member of the Society for Molecular Imaging, the Academy of Molecular Imaging, the American Association for the Advancement of Science, the American Association for Cancer Research, and the American Medical Association. He was named one of the Top 100 Innovators in the World by the *Technology Review*

Magazine for his research in medical technology in 2002. He received the IEEE Engineering in Medicine and Biology Society Early Career Achievement Award in 2005, and was recognized in 2009 with the Paul F. Forman Engineering Excellence Award from the Optical Society of America for dedication and advancement in undergraduate research education.

References

[1]. Denk W, Strickler JH, Webb WW. Two-photon laser scanning fluorescence microscopy. Science. 1990; 248:73–76. [PubMed: 2321027]

[2]. Gannaway JN, Sheppard CJR. Second-harmonic imaging in the scanning optical microscope. Opt. Quantum Electron. 1978; 10:435–439.

[3]. Barad Y, Eisenberg H, Horowitz M, Silberberg Y. Nonlinear scanning laser microscopy by third harmonic generation. Appl. Phys. Lett. 1997; 70:922–924.

[4]. So PTC, C, Y, Dong, Masters BR, Berland KM. Two-photon excitation fluorescence microscopy. Annu. Rev. Biomed. Eng. 2000; 2:399–429. [PubMed: 11701518]

[5]. Zipfel WR, Williams RM, Webb WW. Nonlinear magic: Multiphoton microscopy in the biosciences. Nat. Biotechnol. 2003; 21:1368–1376.

[6]. Sun CK. Higher harmonic generation microscopy. Adv. Biochem. Eng./Biotechnol. 2005; 95:17–56.

[7]. Silberberg Y. Quantum coherent control for nonlinear spectroscopy and microscopy. Annu. Rev. Phys. Chem. 2009; 60:277–292. [PubMed: 18999997]

[8]. Dantus M, Pestov D, Andegeko Y. Nonlinear optical imaging with sub-10 fs pulses. Biochem. Appl. Nonlinear Opt. Spectroscopy. 2009:197–211.

[9]. Isobe K, Tanaka M, Kannari F, Kawano H, Mizuno H, Miyawaki A, Midorikawa K. Nonlinear optical microscopy and spectroscopy employing octave spanning pulses. IEEE J. Sel. Topics Quantum Electron. Jul-Aug;2010 16(no. 4):767–780.

[10]. Meshulach D, Silberberg Y. Coherent quantum control of two-photon transitions by a femtosecond laser pulse. Nature. 1998; 396:239–242.

[11]. Meshulach D, Silberberg Y. Coherent quantum control of multiphoton transitions by shaped ultrashort optical pulses. Phys. Rev. A. 1999; 60:1287–1292.

[12]. Ogilvie JP, Debarre D, Solinas X, Martin JL, Beaurepaire E, Joffre M. Use of coherent control for selective two-photon fluorescence microscopy in live organisms. Opt. Express. 2006; 14:759–766. [PubMed: 19503394]

[13]. Dela Cruz JM, Pastirk I, Comstock M, Lozovoy VV, Dantus M. Use of coherent control methods through scattering biological tissue to achieve functional imaging. Proc. Nat. Acad. Sci. USA. 2004; 101:16996–17001. [PubMed: 15569924]

[14]. Pillai RS, Boudoux C, Labroille G, Olivier N, Veilleux I, Garge E, Joffre M, Beaurepaire E. Multiplexed two-photon microscopy of dynamic biological samples with shaped broadband pulses. Opt. Express. 2009; 17:12741–12752. [PubMed: 19654680]

[15]. Isobe K, Suda A, Tanaka M, Kannari F, Kawano H, Mizuno H, Miyawaki A, Midorikawa K. Multifarious control of two-photon excitation of multiple fluorophores achieved by phase modulation of ultra-broadband laser pulses. Opt. Express. 2009; 17:13737–13746. [PubMed: 19654781]

[16]. Pastirk I, Dela Cruz JM, Walowicz KA, Lozovoy VV, Dantus M. Selective two-photon microscopy with shaped femtosecond pulses. Opt. Express. 2003; 11:1695–1701. [PubMed: 19466048]

[17]. Xi P, Andegeko Y, Weisel LR, Lozovoy VV, Dantus M. Greater signal, increased depth, and less photobleaching in two-photon microscopy with 10 fs pulses. Opt. Commun. 2008; 281:1841–1849.

[18]. Schön P, Behrndt M, Aït-Belkacern D, Rigneault H, Brasselet S. Polarization and phase pulse shaping applied to structural contrast in nonlinear microscopy imaging. Phys. Rev. A. 2010; 81:013809.

[19]. Xi P, Andegeko Y, Pestov D, Lozovoy VV. Two-photon imaging using adaptive phase compensated ultrashort laser pulses. J. Biomed. Opt. 2009; 14:014002. [PubMed: 19256690]

[20]. Dudley JM, Genty G, Coen S. Supercontinuum generation in photonic crystal fiber. Rev. Modern Phys. 2006; 78:1135–1184.

[21]. McConnell G, Riis E. Two-photon laser scanning fluorescence microscopy using photonic crystal fiber. J. Biomed. Opt. 2004; 9:922–927. [PubMed: 15447012]

[22]. Palero J, Boer V, Vijverberg J, Gerritsen H, Sterenborg HJ. Short-wavelength two-photon excitation fluorescence microscopy of tryptophan with a photonic crystal fiber based light source. Opt. Express. 2005; 13:5363–5368. [PubMed: 19498530]

[23]. Isobe K, Watanabe W, Matsunaga S, Higashi T, Fukui K, Itoh K. Multispectral two-photon excited fluorescence microscopy using supercontinuum light source. Jpn J. Appl. Phys. 2005; 44:L167–L169.

[24]. Li D, Zheng W, Qu JAJ. Two-photon autofluorescence microscopy of multicolor excitation. Opt. Lett. 2009; 34:202–204. [PubMed: 19148255]

[25]. Tada J, Kono T, Suda A, Mizuno H, Miyawaki A, Midorikawa K, Kannari F. Adaptively controlled supercontinuum pulse from a microstructure fiber for two-photon excited fluorescence microscopy. Appl. Opt. 2007; 46:3023–3030. [PubMed: 17514253]

[26]. Tu H, Liu Y, Lægsgaard J, Sharma U, Siegel M, Kopf D, Boppart SA. Scalar generalized nonlinear Schrödinger equation-quantified continuum generation in an all-normal dispersion photonic crystal fiber for broadband coherent optical sources. Opt. Express. 2010; 18:27872–27884. [PubMed: 21197060]

[27]. Tu H, Liu Y, Turchinovich D, Boppart SA. Compression of fiber supercontinuum pulses to Fourier-limit in high numerical-aperture focus. Opt. Lett. 2011; 36:2315–2317. [PubMed: 21686005]

[28]. Tu H, Liu Y, Lægsgaard J, Turchinovich D, Siegel M, Kopf D, Li H, Gunaratne T, Boppart SA. Cross-validation of theoretically quantified fiber continuum generation and absolute pulse measurement by MIIPS for a broadband coherently controlled optical source. Appl. Phys. B. 2011 in press.

[29]. Xu B, Gunn JM, Dela Cruz JM, Lozovoy VV, Dantus M. Quantitative investigation of the multiphoton intrapulse interference phase scan method for simultaneous phase measurement and compensation of femtosecond laser pulses. J. Opt. Soc. Amer. B. 2006; 23:750–759.

[30]. Hashimoto H, Isobe K, Suda A, Kannari F, Kawano H, Mizuno H, Miyawaki A, Midorikawa K. Measurement of two-photon excitation spectra of fluorescent proteins with nonlinear Fourier-transform spectroscopy. Appl. Opt. 2010; 49:3323–3329. [PubMed: 20539351]

[31]. Bestvater F, Spiess E, Stobrawa G, Hacker M, Feurer T, Porwol T, Berchner-Pfannschmidt U, Wotzlaw C, Acker H. Two-photon fluorescence absorption and emission spectra of dyes relevant for cell imaging. J. Microscopy. 2002; 208:108–115.

[32]. Laiho LH, Pelet S, Hancewicz TM, Kaplan PD, So PTC. Two-photon 3-D mapping of ex vivo human skin endogenous fluorescence species based on fluorescence emission spectra. J. Biomed. Opt. 2005; 10:024016. [PubMed: 15910090]

[33]. Chen SY, Wu HY, Sun CK. *In vivo* harmonic generation biopsy of human skin. J. Biomed. Opt. 14:060505–2009. [PubMed: 20059236]

[34]. Freudiger CW, Min W, Holtom GR, Xu B, Dantus M, Xie XS. Highly specific label-free molecular imaging with spectrally tailored excitation-stimulated Raman scattering (STE-SRS) microscopy. Nat. Photon. 2011; 5:103–109.

[35]. Lozovoy VV, Dantus M. Coherent control in femtochemistry. Chemphyschem. 2005; 6:1970–2000. [PubMed: 16208734]

[36]. Makarov NS, Drobizhev M, Rebane A. Two-photon absorption standards in the 550–1600 nm excitation wavelength range. Opt. Express. 2008; 16:4029–4047. [PubMed: 18542501]

[37]. Unruh JR, Price ES, Molla RG, Stehno-Bittel L, Johnson CK, Hui R. Two-photon microscopy with wavelength switchable fiber laser excitation. Opt. Express. 2006; 14:9825–9831. [PubMed: 19529374]

[38]. Weiner, AM. Ultrafast Optics. Wiley; Hoboken, NJ: 2009.

[39]. Schibli TR, Kuzucu O, Kim JW, Ippen EP, Fujumoto JG, Kaertner FX, Scheuer V, Angelow G. Toward single-cycle laser systems. IEEE J. Sel. Topics Quantum Electron. Jul-Aug;2003 9(no. 4):990–1001.

[40]. von Vacano B, Motzkus M. Time-resolving molecular vibration for microanalytics: Single laser beam nonlinear Raman spectroscopy in simulation and experiment. Phys. Chem. Chem. Phys. 2008; 10:681–691. [PubMed: 19791452]

[41]. Rehbinder J, Pohling C, Buckup T, Motzkus M. Multiplex coherent anti-Stokes Raman microspectroscopy with tailored Stokes spectrum. Opt. Lett. 2010; 35:3721–3723. [PubMed: 21081975]

[42]. Kano H, Hamaguchi HO. *In-vivo* multi-nonlinear optical imaging of a living cell using a supercontinuum light source generated from a photonic crystal fiber. Opt. Express. 2006; 14:2798–2804. [PubMed: 19516414]

[43]. Selm R, Winterhalder M, Zumbusch A, Krauss G, Hanke T, Sell A, Leitenstorfer A. Ultrabroadband background-free coherent anti-Stokes Raman scattering microscopy based on a compact Er:fiber laser system. Opt. Lett. 2010; 35:3282–3284. [PubMed: 20890360]

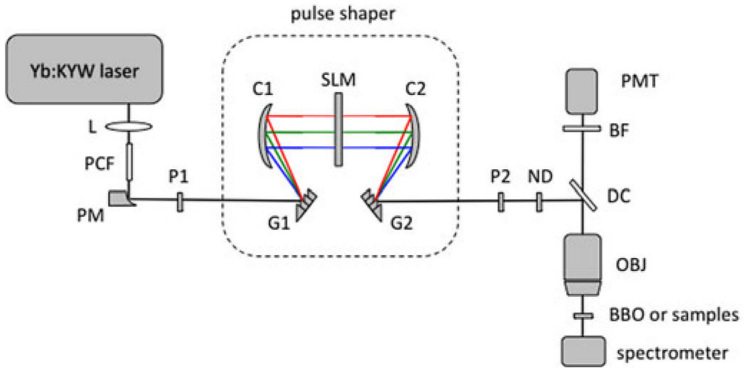

Fig. 1.

Schematic of the experimental setup. BBO: beta barium borate crystal; BF: bandpass filter; C: concave mirror; DC: dichroic mirror; G: diffraction grating; KYW: potassium yttrium tungstate; L: lens; ND: neutral density filter; OBJ: objective; P: linear polarizer; PCF: photonic crystal fiber; PM: parabolic mirror; PMT: photomultiplier tube; SLM: spatial light modulator; Yb: ytterbium.

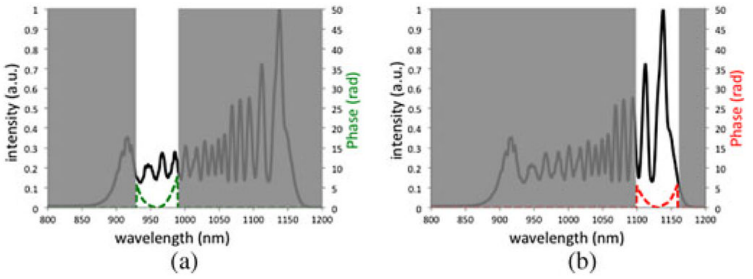

Fig. 2.

Schematic of pulse shaping strategy. The spectrum of the fiber SC (black line), the wavelengths blocked by amplitude shaping (shaded areas), and the measured spectral phase (dashed colored lines) are shown for (a) green (930–990 nm) and (b) red (1100–1160 nm) pulses. A spectral phase opposite to the one measured was introduced by the pulse shaper to compress each color or pulses.

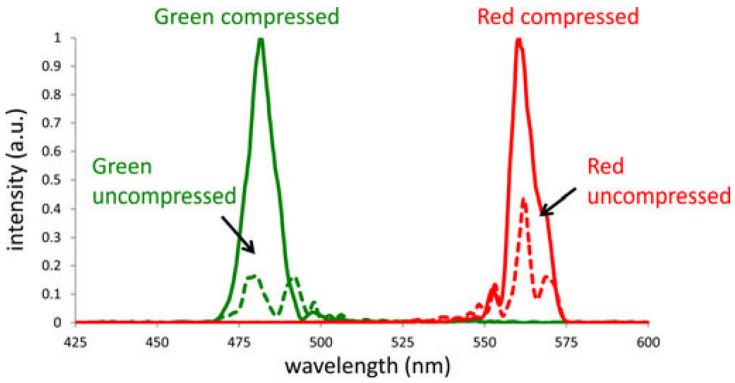

Fig. 3.

SHG spectra of green compressed (solid green), green uncompressed (dashed green), red compressed (solid red), and red uncompressed (dashed red) pulses. By pulse compression, the SHG signal was enhanced by 4.4- and 2.8-fold for green and red pulses, respectively.

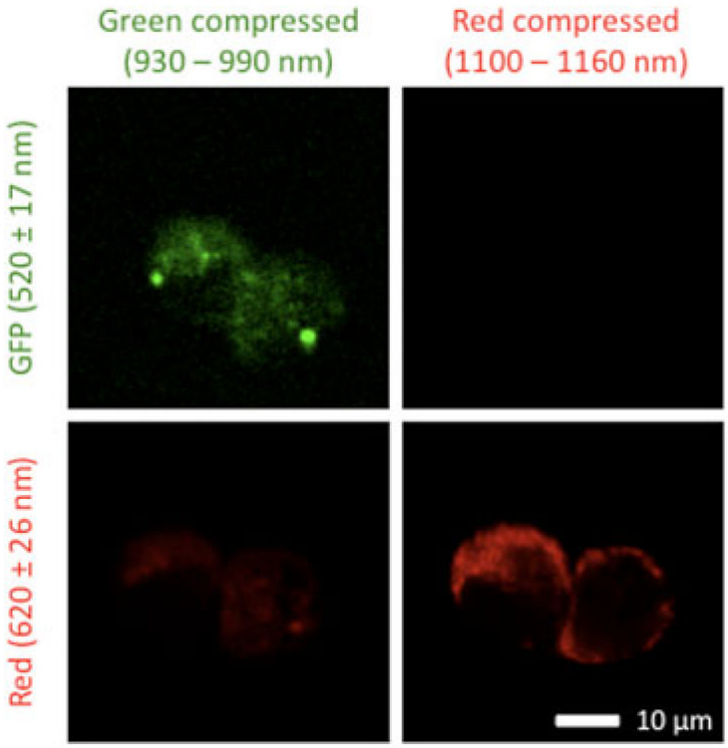

Fig. 4.

TPF images of GFP-transfected fibroblasts costained with Mitotracker Red CMXRos acquired in different detection channels (rows) by illuminating with different compressed pulses (columns). In the GFP channel, the fluorescence intensity of green compressed pulses is high while that from red compressed pulses is low. In the red channel, the opposite is observed. The images demonstrate selective excitation of GFP and Mitotracker Red CMXRos by green and red compressed pulses, respectively.

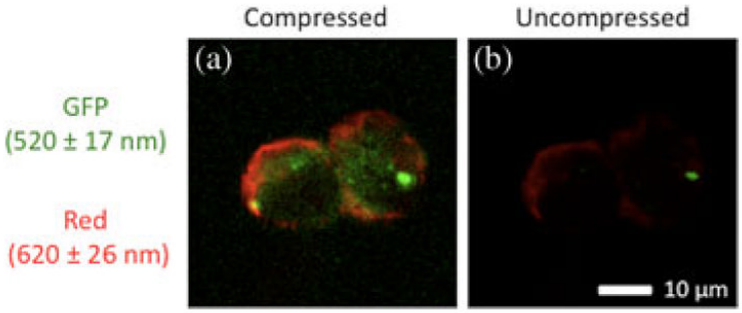

Fig. 5.

TPF images of GFP-transfected fibroblasts costained with Mitotracker Red CMXRos acquired with (a) compressed and (b) uncompressed pulses. The image in (a) is a merged image from the green compressed pulses in the GFP channel and red compressed pulses in the red channel. Image (b) is from uncompressed control pulses. By pulse compression, the fluorescence intensity is enhanced by 3.6- and 3.2-fold for green and red signals, respectively.

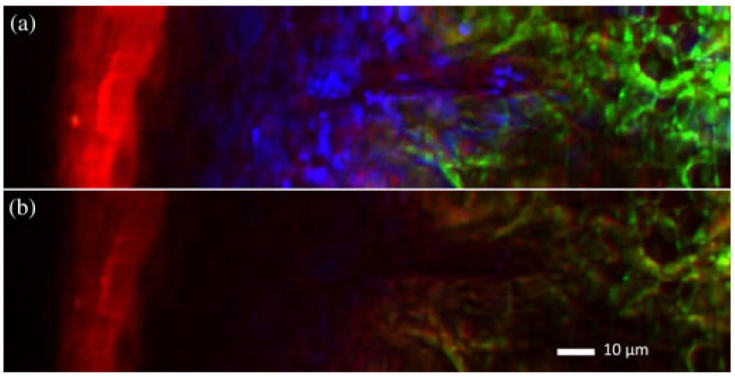

Fig. 6.
Label-free multimodal nonlinear optical imaging of porcine skin acquired with (a) compressed and (b) uncompressed pulses. TPF, SHG, and THG are represented in red, green, and blue pseudocolor. By pulse compression, TPF, SHG, and THG signals were enhanced by 1.9-, 2.4-, and 8.5-fold, respectively.